Transactions of the Nigerian Association of Mathematical Physics
Volume 10, **(***July and November, 2019***), pp185 – 188**

BAND GAP NARROWING AND URBACH ENERGY INCREMENT OF TITANIUM DIOXIDE USING SILVER NANOPARTICLES

Onimisi M. Y[1], Eli D[1,5]*, Garba S[2], Jamila T[3], Ibeh G. J[1], Ige O. O[1] and Lucky E[4]

[1]Department of Physics, Nigerian Defence Academy, Kaduna, Nigeria.
[2]Department of Chemistry, Nigerian Defence Academy, Kaduna, Nigeria
[3]Department of Physics, Kaduna State University, Kaduna, Nigeria.
[4]Department of Chemical Sciences, Greenfield University, Kaduna, Nigeria.
[5]Department of Physics, Greenfield University, Kaduna, Nigeria.

Abstract

Titanium dioxide (TiO_2) incorporated with silver nanoparticles (AgNPs) was synthesized and investigated. The incorporation of silver nanoparticles caused the absorption edge of TiO_2 to be shifted into the lower-energy region. A decrease in band gap energy from 3.23 eV to 2.19 eV was observed when TiO_2 was modified with Ag@P_4VP NPs. Also, at the point when the AgNPs was modified with P_4VP, the band gap energy diminished from 2.03 eV to 1.96 eV. We also observed an increase in urbarch energy from 515 to 546 meV when silver nanoparticles was introduced, which indicates a considerable introduction of tail states at the band edge thus influencing the electron transport in the film. This increase could be attributed to the increase in the defect density due to the incorporation of AgNPs@P_4VP and increase of oxygen vacancy atoms within the TiO_2 film.

***Keywords*:** silver nanoparticlesurbarch energy, electron transport, defect density, oxygen vacancy.

1. Introduction

The large energy band gap of TiO_2inhibits it from being active under UV light [1-3]. The solar spectrum is made up of only 3–5% UV light and around 40% visible light [3]. Therefore, the efficiency of TiO_2 as a photocatalyst under sunlight irradiation is limited. Modification of TiO_2 to improve the photocatalytic efficiency of TiO_2 under sunlight visible irradiation is necessary.

In previous studies, in order to improve the photoreactivity of TiO_2 and to extend its absorption edge into the visible-light region, doping of various transition metal cations has been investigated extensively [4-7]. Except for a few cases [6,7], however, the photoactivity of the cation-doped TiO_2 decreased even in the UV region. This is because the doped materials suffer from a thermal instability or an increase in the carrier-recombination centers [4].

Umebayashi et al. [8] demonstrated the doping of TiO_2 with S atoms. From the result they obtained, S atoms occupied O-atom sites in TiO_2 to form Ti-S bonds. The S doping caused the absorption edge of TiO_2 to be shifted into the lower-energy region.

Some groups have demonstrated the substitution of a nonmetal atom such as nitrogen (N) [9–12] and fluorine (F)[13-15] for oxygen (O). Lee *et al.* [8] fabricated the N-doped TiO_2 films on a silicon substrate by metalorganic chemical vapor deposition using titanium tetra-isopropoxide and nitrous oxide. It was shown by Asahi *et al.* [11,12] that N doping shifted the absorption edge to a lower energy, thereby increasing the photoreactivity in the visible-light region. On the other hand, F doping in TiO_2 was carried out by gas-phase HF treatment at high temperatures [13], a sol–gel technique [14] and ion implantation [15]. The photocatalytic performance of the F-doped TiO_2 was enhanced due to reduction of the recombination rate of the photo generated charge carriers [14].

In contrast, we expected that the introduction of silver nanoparticles could significantly modify the electronic structures of TiO_2 because AgNPs has a larger ionic radius compared to previously used materials. However, there have been reports regarding AgNPs incorporation into TiO_2 by Serry et al. [3] which shows an effective photocatalytic material (6–50% improvement in catalytic efficiency), which is attributed to the fact that the silver is homogeneously dispersed throughout the material. Also the effect of Ag doping on titania and its photocatalytic activity by UV irradiation was studied by Chao et al. [15] (by the sol–gel method) and they found that Ag doping promotes the anatase to rutile transformation, which is attributed to the increase in specific surface area which causes the improvement in photocatalytic activity, and enhances the electron–hole pair separation.

There are some contradictory results also reported showing the decreased activity of silver modified titania[16,17].This may be due to their preparation method, nature of organic molecules, photoreaction medium, or the metal content and its dispersion. Even though there are many studies showing the photocatalytic activity of silver doped titania[16, 18-20], the exact mechanism and the role of silver is under debate. In this paper we report a systematic study of solar initiated photocatalytic activity of spin coated titania with silver nanoparticles. We discussed the effect on the optical-response properties and the result shows that the introduction of silver nanoparticle into the TiO_2enhances the optical-response and contributes to the band gap narrowing and increased urbarch tailing.

2.Experimental section

2.1 Preparation of TiO_2 Paste

The TiO_2 films was prepared using a modified sol–gel technique, in which 3 g of P25 (Dagusta) TiO_2 powder was dissolved in 15 ml of deionized water blended with 0.3 mol of Triton-X 100 and 0.5 g of acetaldehyde, and then vibrated ultrasonically for 24 hours.

Correspondence Author: Eli D., Email: danladielibako@gmail.com, Tel: +234806337256

2.2 Synthesis of Ag nanoparticles

To fabricate the silver NPs, a modified two-step reduction synthesis procedure was implemented, which was developed based on the conventional reduction method which was described in our previous studies [16]. We first heat the mixture containing sodium borohydride ($NaBH_4$) and tri-sodium citrate (TSC) at the ratio of 2:7 ($1x10^{-3}$ mol dm^{-3}: $3.5x10^{-3}$ mol dm^{-3}) to 60 ºC at 300 rpm for 30 minutes under vigorous stirring to ensure a formation of homogenous solution. 45 minutes later, 4 ml of an aqueous solution of $AgNO_3$ ($4x10^{-3}$ mol dm^{-3}) was added drop-wise to the mixture, and the temperature was further raised to 100 ºC to make the solution boil quickly. The reaction was allowed to continue for another 45 minutes. Finally, the solution was cooled down to room temperature with stirring, and the NPs were collected by centrifugation at 5000 rpm and redispersed in ethanol via sonication for 15 minutes.

2.3Preparation of Ag@P_4VP

An aqueous solution of P_4VP was introduced to the silver already synthesized in section 2.2, it follows with modification of the surface with acetone. To hasten the reaction process, P_4VP coating, the solution was stirred for 12hrs at room temperature using a magnetic stirrer. The P_4VP coating silver NPs are collected by centrifugation and redispersed in deionized water by sonication.

2.4Preparation of TiO_2/AgNPs

The glass slides were cleaned using cotton wool soaked in sodium laury sulfate. It was then sonicated in a sonicator for 1 minute to remove excess impurity. It was rinsed with distilled water to evacuate excess fumes. The glass slides were dried after cleaning, with magnetic stirrer plate 78-1 (PEC medicals, USA) at 76 ºC. The temperature was observed using an infrared thermometer for 5 minutes.

The TiO_2 liquid paste was spin coated on the glass slide substrate at the speed of 3000 rpm for 20 seconds. The deposited TiO_2 were dried at 150 °C for 5 minutes. With this one-advance sintering process, it was sintered at 450 °C for 30 minutes, which was advantageous to the enhancement of the interfacial contact. Silver nanoparticles (AgNPs) were deposited through successive ionic layer adsorption and reaction (SILAR) procedure. Numerous strategies, both chemical and physical classes, including, wet chemical [21], polyol process [22], seed-mediated growth [23], photochemical [24], sonochemical [25], electrochemical [26], bioinspired [27], sputtering [28], and laser ablation [29], which have been, hitherto, reportedly employed to synthesize various plasmonic Ag nanostructures, possess one disadvantage or the other, such as toxic reducing agents, impurities, organic solvents, or may require special condition like high-temperature or low-pressure environment, and sometimes expensive and time-consuming procedures may be involved [30].

One of the newest solution methods of deposition techniques for the demonstration of thin film is SILAR method, or, in other words known as modified chemical bath deposition (CBD). SILAR method is relatively simple and offers wide range of advantages over other expensive methods of thin film deposition. It offers simple, inexpensive, and time-saving procedures, which can be carried out at room temperature with no restrictions onsubstrate material, dimensions or its surface profile, and the thickness of the film or nanoparticle can be easily controlled [31-34]. Because of the above advantages, the SILAR technique was used for depositing our AgNPs.

2.5Preparation of TiO_2/Ag@P_4VP NPs

Considering the melting point of P_4VP polymer which is considered to be less than the annealing temperature for TiO_2 by a factor ~ 2.65, and with the expectation of dispersing the Ag@P_4VP NPs into the TiO_2 layer homogeneously, direct spin coating is utilized. The Ag@P_4VP NPs in ethanol solution was onto the TiO_2 layer deposited at the condition of 3000 rpm for 20 seconds, followed by natural drying to expel the ethanol.

2.6Characterization and Measurement

The optical properties and band gap of the functionalized materials were obtained using UV-Visible spectrophotometry (Axiom Medicals UV752 UV-vis-NIR), to predict the charge exchange possibility between the acceptor and donor.

3.Results and Discussion

3.1 Evaluation of band gap energy (Eg) of TiO_2,AgNPs, AgNPs@P_4VP, TiO_2/Ag@P_4VP

Energy band gap of prepared samples have been evaluated from absorption spectra. The absorption coefficients as a function of photon energy for direct and indirect optical transitions aredemonstrated in the figures below:

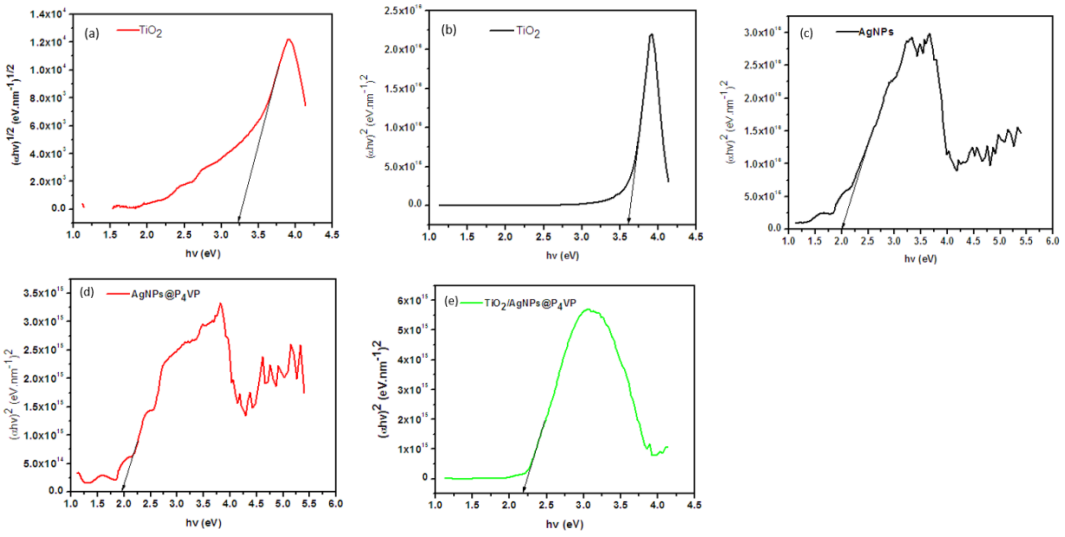

Figure 1: The plot of (a) $(\alpha h\nu)^{1/2}$ vs photon energy for TiO_2, (b) $(\alpha h\nu)^2$ vs photon energy for TiO_2, (c) $(\alpha h\nu)^2$ vs photon energy for AgNPs, (d) $(\alpha h\nu)^2$ vs photon energy for AgNPs@P_4VP and (e) $(\alpha h\nu)^2$ vs photon energy for TiO_2/AgNPs@P_4VP.

The optical band gap Eg was estimated from the following relation, which is known as the Tauc plot [35]:

$$(\alpha h\nu) = B(h\nu - E_g)^n \quad (7)$$

Where, B is a constant, *v* is the transition frequency and the exponent *n* describes the nature of band transition. n = 1/2 and 3/2 corresponds to direct allowed and direct forbidden transitions and n = 2 and 3 corresponds to indirect allowed and indirect forbidden transitions, respectively. When, in this transition, the electron momentum is conserved, the transition is direct, but if the momentum does not conserve this transition it must be attended by a photon, this is an indirect transition [36,37].

The band gap can be obtained from extrapolation of the straight-line portion of the (α hν)^{2}vshν or (α hν)$^{1/2}$vshνplot to $h\nu$= 0.

$\alpha$is the absorption coefficient that can be calculated from absorbance spectra given as:

$$\alpha = \frac{2.303A}{d} \quad (8)$$

Where *d* is the thickness and *A* is the absorbance.

We utilized ISolution Image Analysis programming to measure the thickness of the film to be 50 nm for TiO_2, 70 nm for TiO_2/Ag@P_4VP and 16 nm for AgNPs.

The relation of the absorption coefficient to the incidental photon energy depends on the type of electronic transition (direct or indirect transition).

Figures 1(a-e) demonstrates the Tauc plot of (αhν)^{2}against *h*vand (α hν)$^{1/2}$ against hv of TiO_2, AgNPs, AgNPs@P_4VP, and TiO_2/AgNPs films. The optical direct and indirect energy band gap of the as prepared TiO_2 films were evaluated at the intercept of zero y-axis of linear extrapolation of the plot to enable us know whether the most ideal transition for the functionalized nanoparticle is direct or indirect. The estimated direct and indirect band gaps are observed to be 3.60 eV and 3.23 eV. While the direct band gap for AgNPs is 2.03 eV. At the point when the AgNPs was modified with P_4VP, the band gap energy reduced to 1.96 eV. A decrease in band gap energy from 3.23 eV to 2.19 eV was observed when TiO_2 was modified with Ag@P_4VP NPs. This decrease in energy band gap may be attributed to an increase in grain size due to increase in film thickness. This has essentially established quantum measure impact whereby the smaller the grain sizes the higher the energy band gap [38]. The decrease in the band gap energy, permit AgNPs@P_4VP, and TiO_2/Ag@P_4VP NPsphoto catalyst to be active in the visible region. The absorption shift might be as a result of diffusion of the metallic silver into the crystal lattices of the TiO_2 structure.

Result obtain from the plot, indicates that the indirect transition of TiO_2 is 3.23 ev. This result is contrary to the work of Reddy et al[39].This could be infered that the indirect transition is more favourable for TiO_2 nanoparticles with anatase phase which is in agreement with past reports for anatase TiO_2 [40,41]. The direct transition demonstrated an unrealizable bandgap estimation of 3.60 eV, since its only amorphous material that the band gap is greater than 3.40 eV independent of the transition types.

3.2 Assessment of Urbach Energy

In optical absorption in a semiconductor, electrons get energized over the energy band gap from the highest point of the valence band (VB) to the base of the conduction band (CB). When the encounter disorder during this transition, the electrons experience issue. As a result of this change, their density of states diminish exponentially (tail off) into the energy band far from CB. This tail of density of states reaching out into the energy band gap is termed urbach tail and the energy related with it is the urbach energy. Swanepoel [42], and caglar [43], reported that absorption coefficient (α) near the band edge assume an exponential dependence on photon energy estimated by following equation:

$$\alpha = \alpha_0 \exp(h\nu / E_U) \quad (9)$$

The values of urbach energy were calculated from the plot of ln(α) versus photon energy (hv) for TiO_2 and TiO_2/AgNPs@P_4VP films. The plot is governed by equation (10)

$$\ln(\alpha) = \ln(\alpha_0) + h\nu / Eu \quad (10)$$

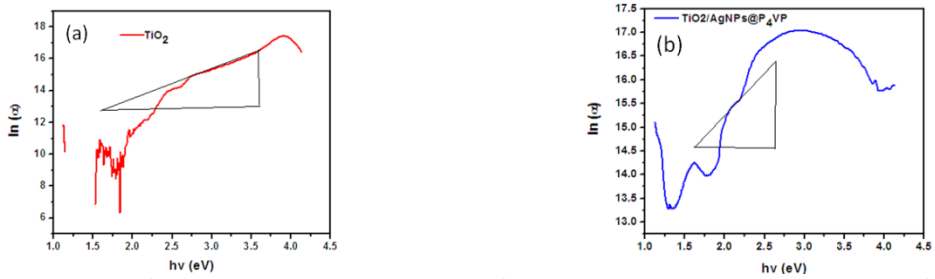

Figure 2: Plot of (a) ln(α) versus photon energy (hv) for TiO_2 (b) ln(α) versus photon energy (hv) for TiO_2/AgNPs@P_4VP film.

The reciprocal gradient of the linear portion of the curve was used to calculate the urbach energy and a value of 515 meV was obtained for TiO_2 and 546 meV for TiO_2/AgNPS@P_4VP as shown in figure 2. The values of eV can be used to measure structural disorder in the prepared samples. The urbach energy of 515 and 546 meV indicated that there was considerable introduction of tail states at the band edges thus influencing the electron transport in the films.

The presence of urbach tail is because of the structure, caused by the deformities and doping in the thin films [44]. The increase in E_U suggests that the atomic structural disorder of studied films increase. The introduction of Ag@P_4VP NPs remarkably increases the urbach energy value, in agreement with others using different materials for doping [45,46]. Such increment could be identified with the increase in the imperfection in surface density because of the incorporation of Ag@P_4VP NPs and increment of oxygen vacancy within the TiO_2 molecules inside the TiO_2 film [47,48], which suggests the likelihood of long range order, locally emerging from the formation of a bond between the TiO_2 and the Ag@P_4VP NPs. In TiO_2 nanoparticles, Ti^{4+} is surrounded by six oxygen ions forming basic $TiO6^{2-}$ octahedra. Loss of oxygen in the lattice discharges free electrons. These free electrons are either captured by Ti^{4+} to form Ti^{3+} on the lattice site, to maintain charge neutrality, or got captured in the oxygen vacancy. The electrons captured by the Ti^{4+}, on either side of oxygen vacancy (V_0), forms Ti^{3+}-V_0-Ti^{3+} defect complex, and the electrons captured by the oxygen vacancies form color centers (F, F^+ or F^{++}) [49,50]. Subsequently, basic deformities, from sample, such as Ti^{3+} and oxygen vacancies are the reason behind the broadening of the light absorption of TiO_2/Ag@P_4VP NPs upto visible region. Absence of visible absorption peaks in pure TiO_2 does not indicate that this sample is devoid of oxygen vacancies. Oxygen vacancies are present in the sample. But the concentration of these defects may be too low to be detected. The lowering of band gap in TiO_2/AgNPs@P4VP indicates presence of defect bands in the band gap of TiO_2. These defect states produce an absorption tail extending deep into the forbidden gap. This tail is referred as Urbach tail and the associated energy as Urbach energy [51,52].

Addition of AgNPs@P_4VP enhanced the shuffling motion of atoms in composite films. Such unlimited motion could have expanded the urbach tailing thus increasing the eV due to increased number of vibrational energy levels for a given electronic state. The obtained value of E_U was within the range (46 to 660 meV) for semiconductors reported by Staet al. [53]. The urbach energy value of 515 meV obtained in this investigation was noteworthy in showing the introduction of tail states at band edges that impact electron transport.

4. Conclusion

The TiO_2-based nanoparticles incorporated with AgNPs@P_4VP nanoparticles were synthesized using spin coating procedure. The addition of AgNPs@P_4VP nanoparticles was found to cause a significant shift in the absorption edge to lower energy. From the analysis of urbach energy, incorporating AgNPs@P_4VP nanoparticles results to imperfection in surface density and increment of oxygen vacancy within the TiO_2 molecules inside the TiO_2 film, which suggests the likelihood of long range order, locally emerging from the formation of a bond between the TiO_2 and the Ag@P_4VP NPs.

References

[1] Pelaez, M., Nolan, N. T., Pillai, S. C., Seery, M. K., Falaras, P., Konto, A. G., Dunlop, P. S. M., Hamilton, J. W., Byrne, J. A., O'shea, K., Entezari, M. H., Dionysiou, D. D. (2012). *Applied Catalysis B: Environmental*, 125, 331-349.

[2] Seery, M.K., George, R., Floris, P., Pillai, S.C. (2007). Journal of Photochemistry and Photobiology: A Chemistry, 189, 258–263.

[3] Sontakke, S., Mohan, C., Modak, J., Madras, G. (2012). *Chemical Engineering Journal*, **189-190**, 101-107.

[4] Choi, W., Termin, A., and Hoffmann, M. R. (1994). J. Phys. Chem. **98**, 13669.

[5] Herrmann, J. Disdier, M. J. and Pichat, P. (1984). Chem. Phys. Lett. **108**, 618.

[6] Yamashita, H., Ichihashi, Y. Takeuchi, M. Kishiguchi, S. and Anpo, M. (1999). J. Synchrotron Radiat. **6**, 451.

[7] Karakitsou, K. E. and Verykios,X. E. (1993). J. Phys. Chem. **97**, 1184.

[8] Umebayashi, T. Yamaki, T. Itoh, H. and Asai, K. (2002).Appl. Phy. Lett. Vol. 81, No. 3, 454-458.

[9] Lee, D. H., Cho, Y. S., Yi, W. I. Kim,T. S., Lee, J. K., and Jung, H. J. (1995). Appl. Phys. Lett. **66**, 815.

[10] Saha, N. C. and Tompkins,H. G. J. (1992). Appl. Phys. **72**, 3072.

[11] Asahi, R., Morikawa, T., Ohwaki,T.,Aoki,A. and Taga, Y. (2001). Science **293**, 269.

[12] Morikawa, T., Asahi, R., Ohwaki, T., Aoki,A., and Taga, Y. (2001).Jpn. J. Appl. Phys., Part 2 **40**, L561.

[13] Subbarao, S. N., Yun, Y. H., Kershaw, R., Dwinghta, K., and Wold, A. (1979). Inorg. Chem. **18**, 488.

[14] Hattori, A.,Yamamoto, M., Tada, H., and Ito, S. (1998).Chem. Lett., 707.

[15] Chao, H. E., Yun, Y. U., Xiangfang, H. U., Larbot, A. (2003). J. Eur. Ceram. Soc. 23,406, 1457.

[16] Eli, D and Gyuk, P.M. (2019). Sci. World. J. 14(2), 125-130.

[17] Vamathevan, V., Amal, R., Beydoun, D., Low, G., McEvoy, S. (2002). J. Photochem.429 Photobiol. A 148, 233, 430.

[18] Sokmen, M., Allen, D. W., Akkas, F., Kartel, N., Acar, F. (2001).Water, Air Soil 433 Pollut.132, 153.

[19] Sung-suh, H. M., Choi, J.R. ,Hah, H.J., Koo, S.M., Bae, Y.C. (2004). J. Photochem. Photobiol. A 163, 37. 436.

[20] Zhang, L.,Yu, J.C.,Yip, H.Y., Li,Q., Kwong, K.W., Xu,A., Wong, P.K. (2003).Langmuir 19, 437, 10372.

[21] Yang, J., Dennis, R., Sardar, D. (2011). *Materials Research Bulletin*, 46, 1080–1084.

[22] Sadeghi, B., Sadjadi, M., Vahdati, R. (2009). *Superlattices and Microstructures*, 46, 858–863.

[23] Nouneha, K.H., Oyama, M., Diaz, R., Abd-Lefdil, M., Kityk, I., Bousmina, M. (2011). *Journal of Alloys and Compounds*, 509, 2631–2638.

[24] Jia, H., Zeng, J., Song, W., An, J., Zhao, B. (2006). *Thin Solid Films*, 496, 281–287.

[25] Zhu, Y.P., Wang, X.K., Guo, W., Wang, J.G., Wang, C. (2010). *Ultrasonics Sonochemistry*, 17, 675–679.

[26] Reicha, F.M., Sarhan, A., Abdel-Hamid, M.I., El-Sherbi, I.M. (2012). *Carbohydrate Polymers*, 89, 236–244.

[27] Zhang, X., Liu, J., Li, S., Tan, X., Yua, M., Dua, J. (2013). RSC Advances, 3, 18587–18595.

[28] Xiong, Y., Wu, H., Guo, Y., Sun, Y., Yang, D., Da, D. (2000). *Thin Solid Films* 375, 300–302.

[29] Alonso, J., Diamant, R., Castillo, P., AcostaeGarcı´a, M.C., Batina, N., Haro-Poniatowski, E. (2009). *Applied Surface Science*, 255, 4933–4937.

[30] Amiri, M., Nouhi, S., Azizian-Kalandaragh, Y. (2015). *Materials Chemistry and Physics*, 155, 129–135.

[31] Eli, D., Gyuk, P. M., and Oluwaseyi, B. S. (2018). *Nigerian Journal of Physics*, 27(S), 265-272.

[32] Mitzi, D. B. (2009). Wiley, New Jersey.

[33] Isah, K.U. (2008). Nigerian Journal of Physics, 20, 335–339.

[34] Pathan, H.M., Lokhande, C.D. (2004). *Bulletin of Materials Science*, 27(2), 85–111.

[35] *Tauc*, J. (*1974*). Vol. 159. Plenum Press, New York.

[36] Dressel M, Gruner G. (2002). Cambridge University Press, 159-165.

[37] *Willardson*, R., and *Beer*, A.(*1967).* Academic Press, New York, pp. 318-400.

[38] Oztas, M. (2008). *Chinese Physics Letters*, 25(11), 4090-4092.

[39] Reddy, K., Manorama, S., Redd, A. (2002). *Materials Chemistry and Physics*, 78, 239-245.

[40] Xie, Z., Liu, X., Zhan, P., Wang, W., and Zhang, Z. (2013). *AIP advances*, 3(6), 062129-1 -7.

[41] Grigorov, K. G., Oliveira, I.C., Maciel, H. S., Massi, M., Oliveira Jr., M. S., Amorim, J., and Cunha, C.A. (2011). *Surface Science*, 605(7-8), 775-782.

[42] Swanepoel, R. (1983). *Journal of Physics E: Scientific Instruments*, 16, 1214-1222.

[43] Caglar, M., Ilican, S., and Caglar, Y. (2006). *Physica Macedonica*, 56, 49-55.

[44] Caglar, M., Ilican, S., and Caglar, Y. (2009). *Thin solid films*, 517(17), 5023-5028.

[45] de Lima, M. M., and Marques, F. C. (2002). *Journal of non-crystalline Solid*, 299, 605-609.

[46] Hadjadi, A., St'ahel, P., Rocai Cabarrocas, P., Paret, V., Bounouh, Y., and Martin, J. C. (1998). *Journal of Applied Physics*, 83, 830.

[47] Choudhury, A., and Choudhury B. (2014). *Physica E: Low-dimensional systems and nanostructures*, 56, 364-371.

[48] Abdel-Kader, A., Higazy, A., Elkholy, M. (1991). *Journal of Materials science:Materials in Electronics*, 2(4), 204-208.

[49] Komaguchi, K., Maruoka, T., Nakano, H., Imae, I., Ooyama, Y., Harima Y. (2000). *Journal of Physical Chemistry C*, 114(2), 1240–1245.

[50] Kuznetsov, V.N., &Serpone, N. (2009). *Journal of Physical Chemistry C*, 113(34), 15110–15123.

[51] Boubaker, K. (2011). *European Physical Journal Plus*, 126, 10.

[52] Chiodo, L., Lastra, J. M., Iacomino, A., Ossicini, S., Zhao, J., Petek, H., Rubio, A. (2010). *Physical Reviews B*, 82(4), 045207.

[53] Sta, I., Jlassi, M., Hajji, M., Boujmil, M., Jerbi, R., Kandyla, M., Kompitsas, M., and Ezzaouia, H. (2014). *Journal of Sol-Gel Science and Technology*, 72, 421-427.